

Deformations in KCl single crystals by spherical and pyramidal indenter

S. KOBAYASHI, T. OKUI

Department of Mechanical Engineering, Doshisha University, Kamigyoku, Kyoto 602, Japan

S. MIURA

Department of Engineering Science, Kyoto University, Sakyoku, Kyoto 606, Japan

An indentation test, using a steel ball and a diamond quadrangular pyramid indenter, were carried out on the $\{100\}$ cleaved crystal face of KCl single crystals. The dislocation structures and strain hardening around an indent were examined. In addition, macroscopic deformations such as pile-up and the shape of the indent were investigated. It became clear that – because of the anisotropy of these crystals, plastic deformations, the crystals' area and the strain hardening around the indents – are larger in the $\langle 110 \rangle$ direction than in the $\langle 100 \rangle$ direction, and a regular correspondence relation was confirmed, experimentally, between hardness and dislocation density.

1. Introduction

Wear of material which has rather a rough surface proceeds by the invasions or friction produced by sharp asperity tips or wear debris. In order to elucidate the mechanism of wear, it is necessary to have knowledge of the deformation in the materials produced by such invasions or friction. To study these problems, it is useful to study the dislocation level microscopically by using single crystals. In the present study, the microscopic and macroscopic deformations in the surface layer of KCl single crystals were investigated using a steel ball or a Vickers diamond indenter to indent the $\{100\}$ crystal face. Strain hardening and dislocation structures were examined. In addition, the pile-up or sinking around an indent were observed. These experimental results will be useful in understanding the deformation mechanism of the material produced by the invasion brought about by friction.

2. Experimental procedure

2.1. Sample preparation

KCl single crystals were used for the experiments. The specimens were cleaved in the $\{100\}$ face to a size $7.5 \times 15 \times 5$ mm. These specimens were annealed for 10 h in the temperature range 640–740 °C. The dislocation density of the cleaved surface, estimated with number of etch pits per unit area, was reduced to $6 \times 10^7 \text{ m}^{-2}$ by annealing. The chemical composition of the solution used for etching was CH_3COOH 100 ml mixed a few quantity of Br_2 .

2.2. Experimental details

The details of the apparatus used for ball indentation

tests have been described previously [1]. The indentations were made under a load range of 1.0–5.0 N using a 4 mm diameter, steel ball or a diamond pyramidal indenter. The ball indenter was finally ground to produce a surface finish of about $0.05 \mu\text{m}$ c.l.a. A micro Vickers hardness tester was used for the pyramid indentation tests. After indentation the plastic deformations around the indent were examined with surface-profile testing apparatus of the stylus type. Hardness distributions were also measured in the deformed area. The indented surface and its cross-section were etched to reveal the dislocation structure resulting from indentation. All the experiments were carried out in an atmosphere with a temperature of 20 °C and a humidity of 40%, because KCl crystals are hygroscopic and deliquescent.

3. Results and discussion

3.1. Macroscopic deformations

3.1.1. Anisotropy in the shape of the indent

The diagonals in pyramid indentation were oriented in three ways: (a) parallel to $\langle 100 \rangle$ direction, (b) parallel to $\langle 110 \rangle$ direction, and (c) intermediate to these two. Fig. 1 shows the indents formed immediately after releasing a load of 5.0 N in these three cases. It is found that the shape of the indent on the surface alters from a perfect square [2]. The diagonals are shorter by about 5.0% in case a than in case c; and, as this length is used to calculate the Vickers Hardness, H_v , a high H_v value results in this case. Such differences in the shape of the indent are due to crystal anisotropy, and can be understood by considering the mechanism of slip process. Slips of this material occur easily in the $\langle 110 \rangle$ direction, because (as is shown later in Fig. 7) etch pits, which show the activities of

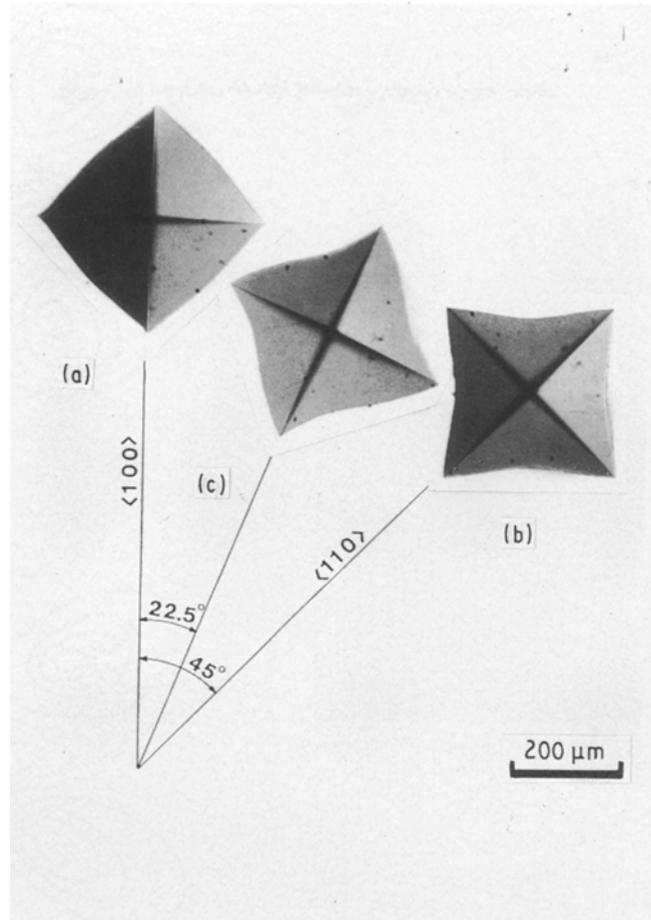


Figure 1 Variation of anisotropy in the shape of indent with direction of indenter (load, 5.0 N).

dislocations, are detected conspicuously in the $\langle 110 \rangle$ direction. That is, KCl single crystals deform more easily in the $\langle 110 \rangle$ direction than in the $\langle 100 \rangle$ direction. The difference in diagonal length with direction corresponds to this anisotropy.

Fig. 2 shows the surface indented with a steel ball under a load of 5.0 N. The shape of an indent is almost square, with diagonals oriented in the $\langle 110 \rangle$ direction. This also indicates that the material can be deformed most easily in the $\langle 110 \rangle$ direction.

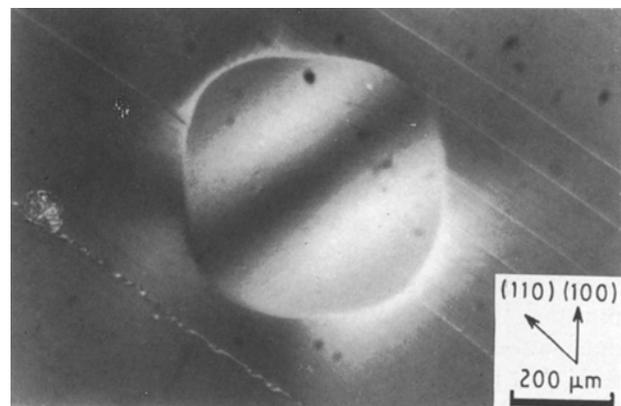


Figure 2 Appearance of the deformation under a 5.0 N indentation.

3.1.2. Topographical deformation around indent

Fig. 3 shows surface topographies, recorded with a surface recorder of stylus type, after loading of pyramidal indenter. Curves a, b, and c were obtained by tracing on the routes A, B, and C, respectively. The occurrence of small hills, due to the piling-up actions of dislocations [3], are observed in each case. The location of the pile-up corresponds to the swollen parts of the sides of the pyramidal indent on the surface. The sinkings of the material, however, are produced where the sides of the indent cave in. Fig. 4 show the contour lines which are obtained by com-

binning the equal-height points in the areas piled-up and sunk-in. The heights of pile-up and sinking are shown in micrometres. There are shades of difference among the contour-line patterns according to the direction of diagonal. The piled-up area was observed in the $\langle 110 \rangle$ azimuth and the sunk-in area was observed in the $\langle 100 \rangle$ azimuth. The maximum length of the ranges of pile-up and sinking are measured as

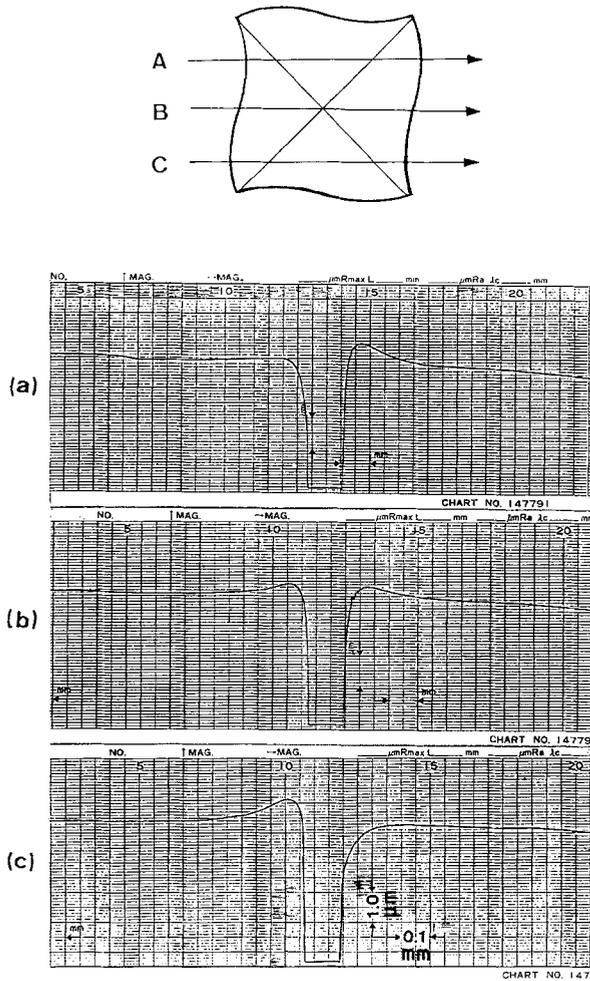


Figure 3 Traces of surface-topography features around indent (load, 2.0 N).

about 300 μm and 200 μm , respectively, and the maximum height of pile-up and sinking are measured as about 8.0 μm and 10.0 μm , respectively.

3.1.3. Strain hardening around indent

The hardness was measured on an indented surface to examine the strain hardening around an indent. Fig. 5 plots hardness versus distance from the centre of the indent. Hardness measured on a cleaved surface before indentation is about $9.3 \pm 0.2(H_v)$, which is shown in Fig. 5 with a chain line. It is clear from this plot that the range of strain hardening produced by indentation is much greater in the $\langle 110 \rangle$ azimuth than the $\langle 100 \rangle$, under a load of both 3.0 and 10.0 N. Hardness increases about 20% or 30% at a distance of 250 μm from the centre of the indent under a load of 3.0 or 10.0 N, respectively. Fig. 6 shows hardness distributions on a cross-section, $\{100\}$, cleaved at the centre of indent. The notch, labelled "A" on the surface level is an indent. The region inside a chain line is strain hardened by indentation. The length, B, which represents the range of hardened area is about 1250 and 2300 μm under loads of 3.0 and 10.0 N, respectively. Hardness beneath the indent increases by about 40% and 50% under these loads. These observed hardness behaviours are considered to be the summation of the effects of pressure during loading, the

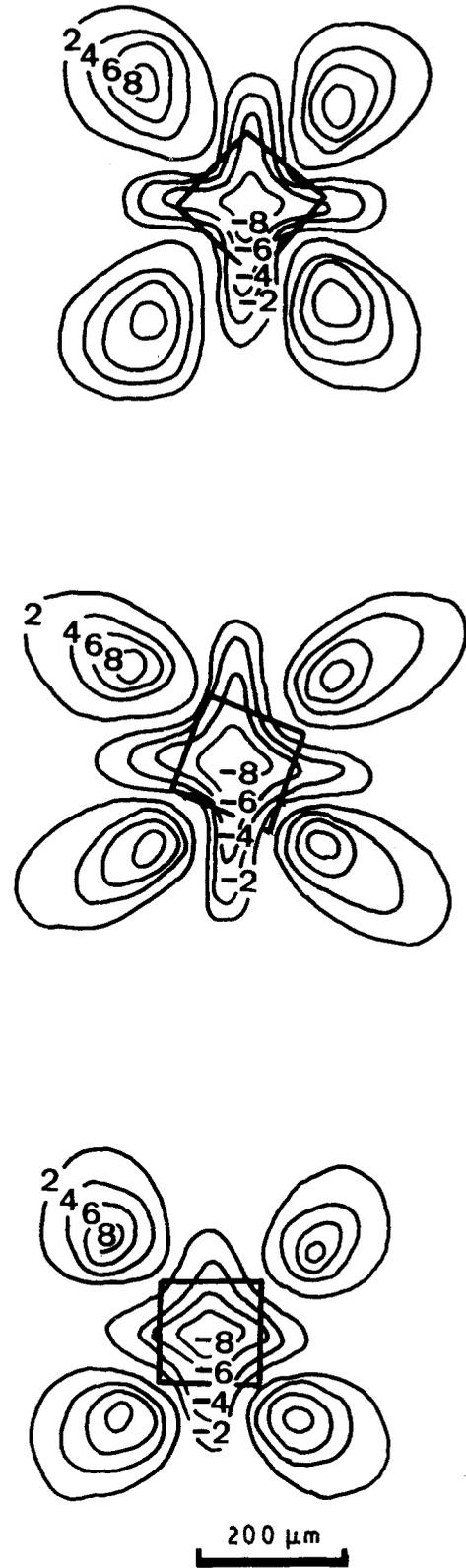


Figure 4 Contour lines (in μm) of Vickers hardness, H_v , around indents (load, 2.0 N).

relaxation of the stress during load removal, and of the residual stress produced during indentation.

3.2. Microscopic deformations

3.2.1. Dislocation-structure pattern

Fig. 7 shows the distribution of dislocations produced by pyramid indentation under a load of 1.0 N. The black centre labelled "A" is an indent. Etch pits

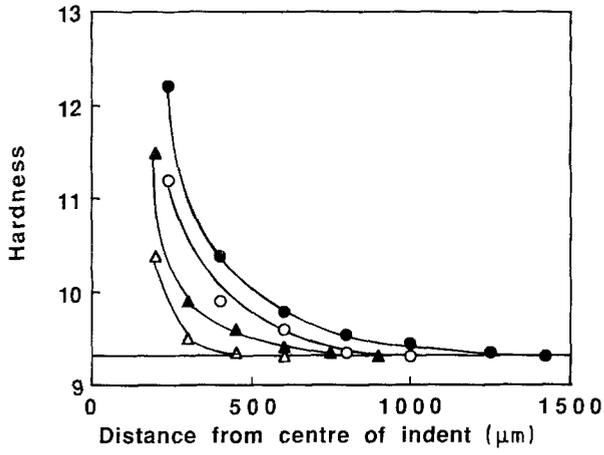


Figure 5 Relations between hardness and distance from the centre of the indent. (Δ) 3.0 N, $\langle 100 \rangle$; (\blacktriangle) 3.0 N, $\langle 110 \rangle$, (\circ) 10.0 N, $\langle 100 \rangle$; (\bullet) 10.0 N, $\langle 110 \rangle$.

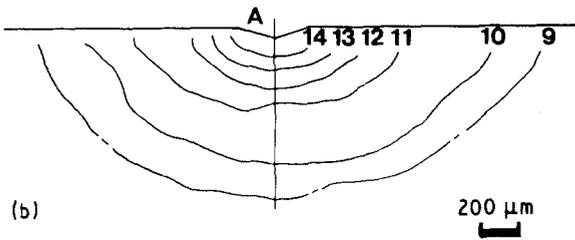
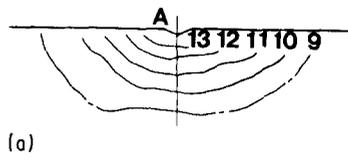


Figure 6 Hardness distributions on cleaved cross-section. (a) load, 3.0 N, (b) load, 10.0 N.

around the indent overlap with each other, and the dislocation density is at a very high level. The dislocation structure forms a wing row pattern which extends in four $\langle 110 \rangle$ directions with comparatively low density. Each row is tapered to the end and bifurcates like a horn at the end part. The average

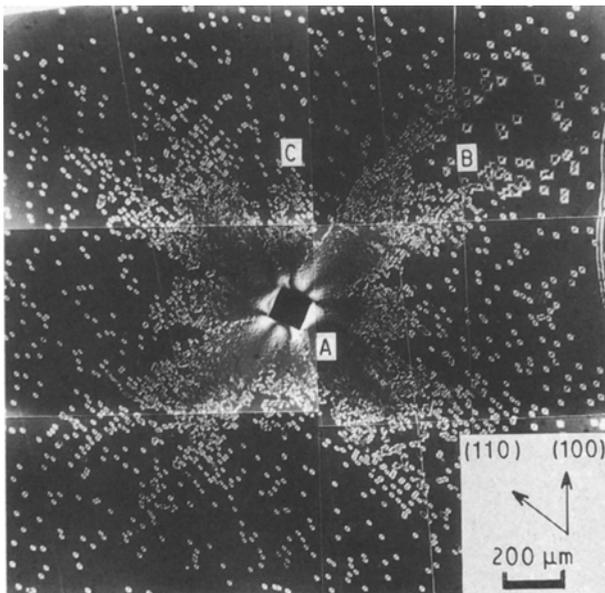
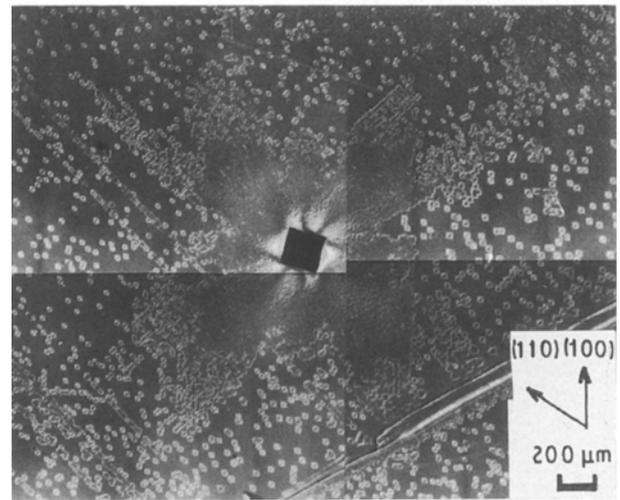
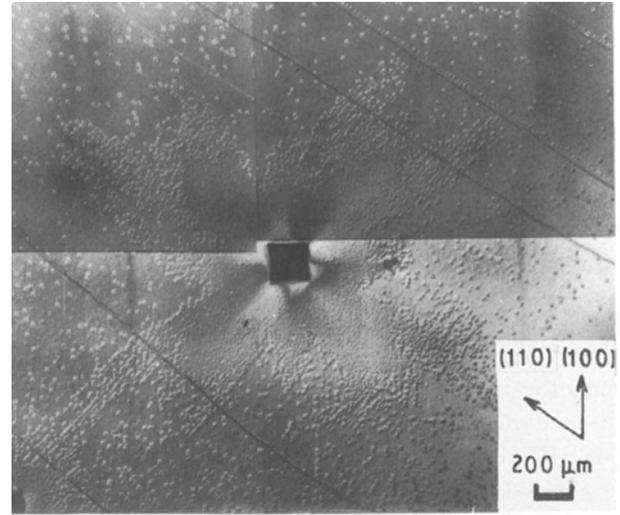


Figure 7 Distribution of dislocations produced by indentation (load, 1.0 N).

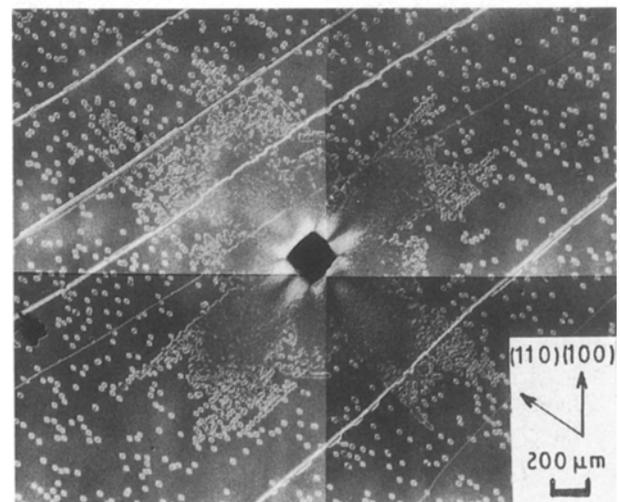


Figure 8 Distribution of dislocations produced by indentation (load, 2.0 N).

length of the rows in the $\langle 110 \rangle$ direction is estimated to reach about three times the maximum length of the range of piled-up area. Increases in hardness due to strain hardening are observed in the range in which the pile-up and sinking of the material are observed. It is found that the distance from the centre of the indent to the border of the strain hardened area is about three times the diameter of an indent, and that the change in hardness is not confirmed in the outer side of its range though dislocations are clearly detected.

Fig. 8 shows the distribution of dislocations produced by pyramid indentation under a load of 2.0 N in three directions of the diagonal. The dislocation-structure patterns are almost similar in the three cases. Compared with the results in Fig. 4, the shape of the combined range of piled-up and sunk areas is almost similar to that of the regions of high dislocation density.

Fig. 9 shows the dislocation-structure pattern obtained under the same load but with a spherical indenter. In this case also, a range with extremely high dislocation density is observed around an indent. Also, the dislocation-structure pattern is quite similar to that for a pyramid indentation.

The slip systems of the KCl crystals are considered to be $\{110\} \langle 110 \rangle$, as has been observed in MgO single crystals [4]. The six slip systems shown in Fig. 10 are considered. Two of these slip planes intersect the indented surface at a right angle, and the other four make an angle of 45° with the surface. Slip directions are labelled in Fig. 10 on these slip planes. These two kinds of planes can be designated as $\{110\}_{90}$ and $\langle 110 \rangle_{45}$, respectively. On these slip planes the dislocation lines form the loops as shown in Fig. 10.

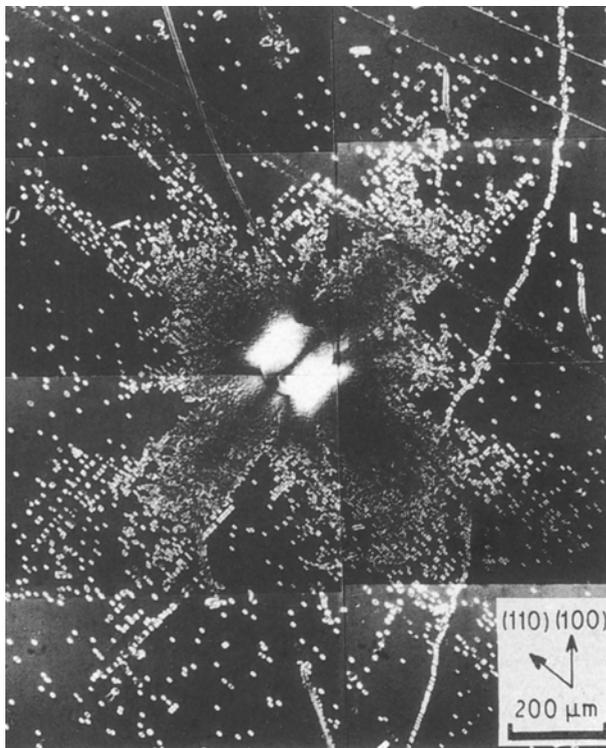


Figure 9 Distribution of dislocations produced by indentation (load, 1.0 N).

3.2.2. Changes in dislocation density due to indentation

Fig. 11 shows the relation between dislocation density and distance from the centre of the indent. At the left side, out of a chain line the number of etch pits cannot be measured because they overlap. As the distance from the centre of an indent increases, the dislocation density decreases monotonically. This decreasing

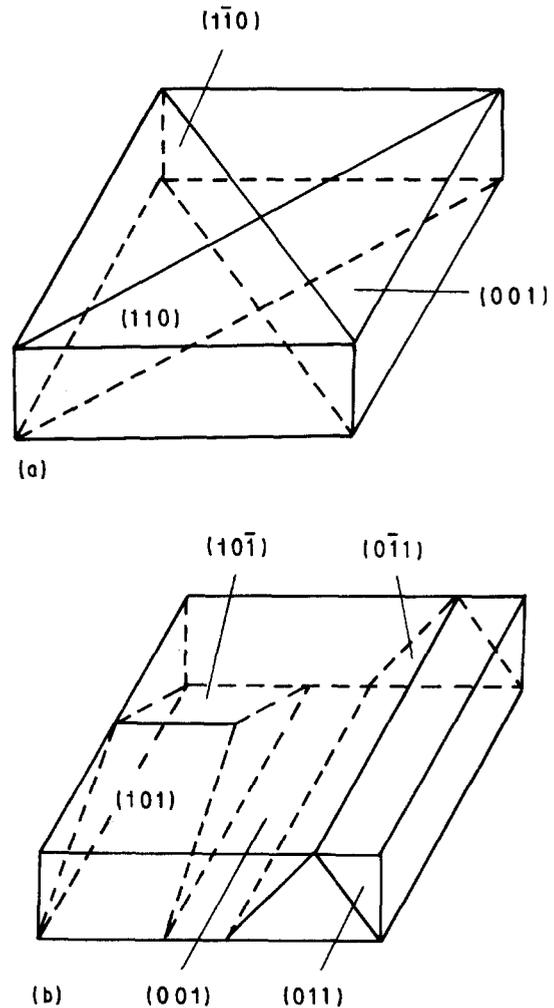


Figure 10 Slip systems in KCl single crystal: (a) $\{110\}_{90}$, (b) $\langle 110 \rangle_{45}$.

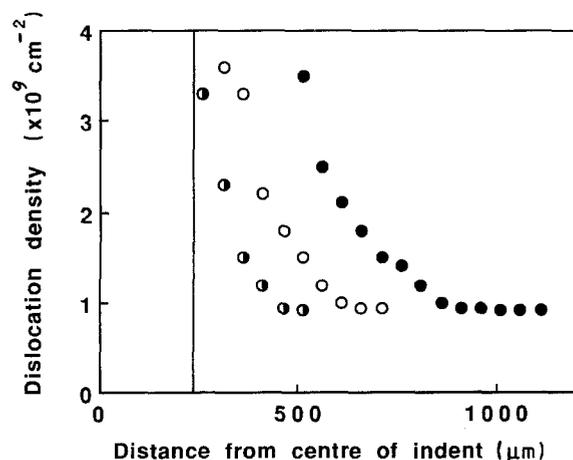


Figure 11 Relation between dislocation density and the distance from the centre of the indent: (●) 0.25 N, (○) 0.5 N, (●) 1.0 N.

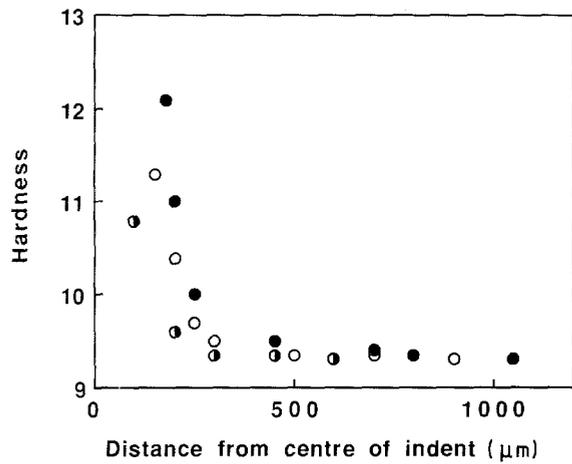


Figure 12 Relation between hardness and distance from centre of indent: (○) 0.25 N, (○) 0.5 N, (●) 1.0 N.

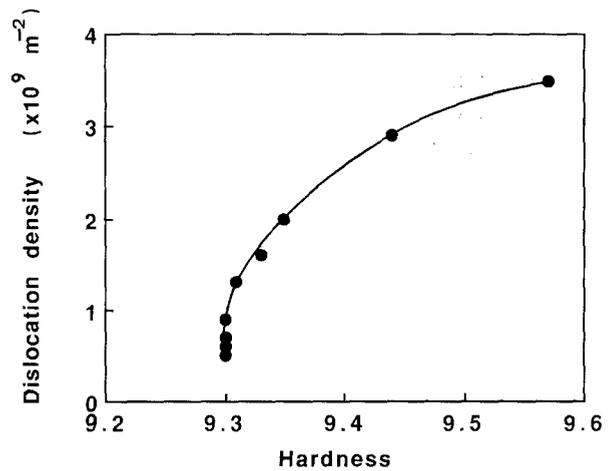


Figure 13 Relation between dislocation density and hardness.

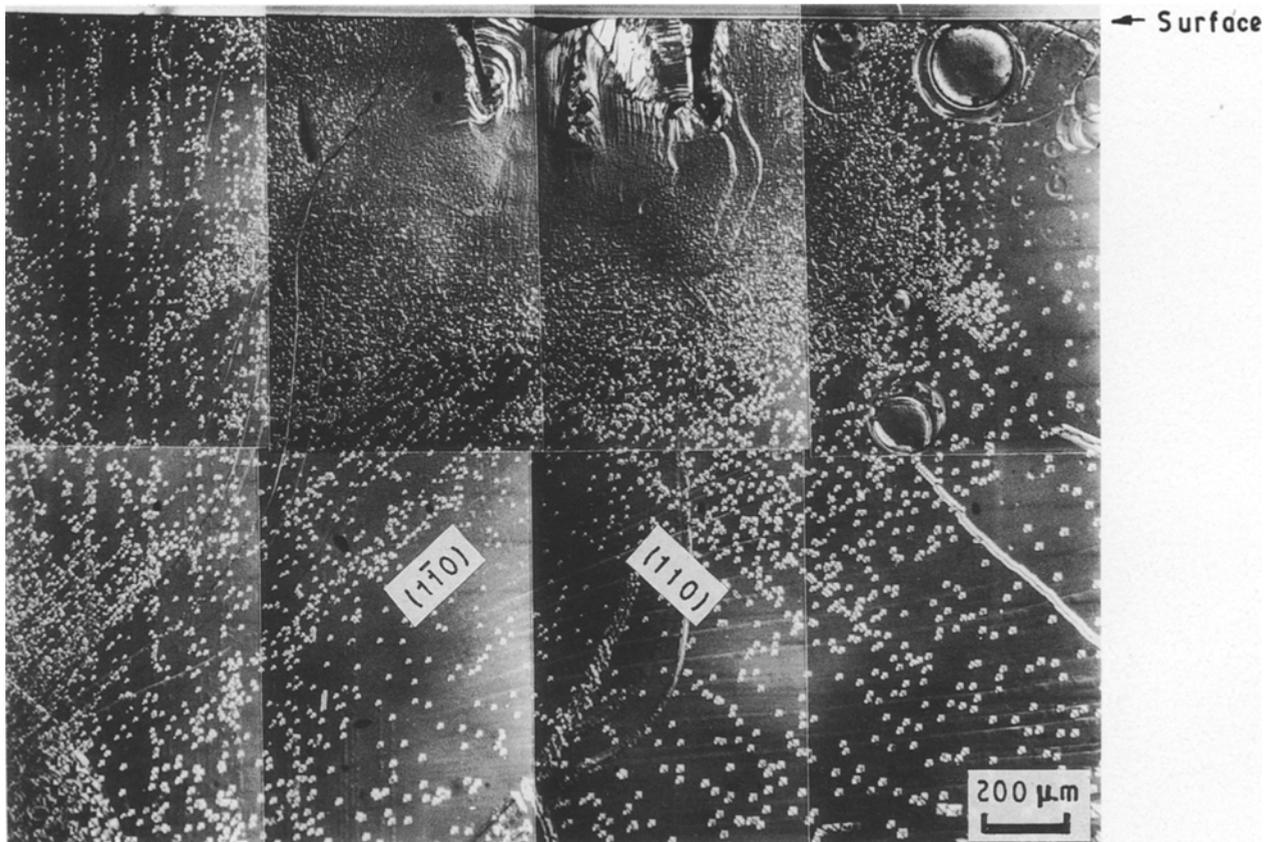


Figure 14 Appearance of deformation on cleaved cross-section (load, 3.0 N).

tendency is similar to the relation between hardness and distance from the center of an indent in Fig. 12. Fig. 13 shows the relation between dislocation density and hardness. The relation shown in this figure does not change with load because dislocation corresponds to hardness. The change in hardness due to indentation is only about 3.0%, whereas the dislocation density shows about an 18-fold change in value from $2.0 \times 10^8 \text{ m}^{-2}$ to $3.6 \times 10^9 \text{ m}^{-2}$.

3.2.3. Observations on cleaved cross-sections
Fig. 14 shows a deformation on a cleaved cross-

section after a 3.0 N pyramid indentation. As the deformation is deep beneath the indent, the condition of the dislocation structure cannot be confirmed. It is found that the dislocation structure forms the pattern of a letter "X", making an angle of 45° to the indented surface in a deeper area than the high-dislocation-density area. And the dislocation structures which make an angle of 90° to the surface are scarcely observed. This shows that dislocation activities are made mainly on the $\{110\}_{45}$ planes in the inside of the crystals.

4. Conclusions

1. The indents formed on surfaces indented with a

ball and a pyramid are not perfectly circular or square because of crystal anisotropy.

2. The appearances of the pile-up and sinking around the indent were clarified.

3. The strain hardening around the indent is more active in the $\langle 110 \rangle$ direction than in the $\langle 100 \rangle$ direction.

4. The deformed area formed on a $\{100\}$ face with a ball or pyramidal indenter consists of a high-dislocation-density range and a wing-shaped area of comparatively low density extending along the $\langle 110 \rangle$ and the $\langle 100 \rangle$ directions.

5. A regular correspondence relation is obtained between hardness and dislocation density.

6. Dislocation activities on the $\{110\}_{90}$ and on the

$\{110\}_{45}$ are mainly detected on the indented surface and on its cross-section, respectively.

References

1. S. KOBAYASHI, T. HARADA and S. MIURA, *J. Mater. Sci.* **26** (1991) 3945.
2. E. AERTS, S. AMELINCKX and W. DEKEYSER, *Acta Metall.* **7** (1959) 29.
3. P. M. SARGENT and T. F. PAGE, *J. Mater. Sci.* **20** (1985) 2388.
4. M. F. AMATEAU and J. W. SPRETNAK, *J. Appl. Phys.* **34** (1963) 2340.

Received 13 March

and accepted 26 October 1992